

# Use of Radical Emission for Determination of Ignition Delay Times

## Behind Reflected Shocks

M. Jelezniak, I. Jelezniak  
Contact: Mark@Jelezniak.de  
15 June 2007

Comments on the work

M. Kalitan, J. M. Hall and E. L. Petersen. Ignition and oxidation of Ethylene-Oxygen-Diluent mixtures with and without silane. *Journal of Propulsion and Power* **21**, No. 6, pp 1045 – 1056, ( 2005)

A method for monitoring ignition processes in shock-heated gas mixtures using emission of radicals is discussed. Integral equations, which relate radiation intensity of the radicals with signals of detectors, are presented. Simple solutions of the equations were obtained for case of transparent gas. These solutions were tested against detector signals from work [1], a good agreement has been achieved. The solutions testify that the use of raw signals of detectors instead of calculated radiation intensity can cause errors in definitions of ignition delay times. For this reason, the results of the work [1], where the ignition delay times are derived from raw signals, are erroneous.

### 1. Introduction

Spectral methods are frequently used to obtain information about heated gases. These methods have advantages; they not disturb the test system and are not inertial. Nevertheless, the reduction of detector signal to parameters of test gas is not always simple and requires processing of raw detector signals. This problem will be discussed here using, as an example, the experimental data from work [1]. In the work [1], ignition delay times  $\tau_{\text{ign}}$  were measured behind reflected shocks in Ethylene-based gas mixtures with and without Silane. The experiments were conducted in a shock-tube facility at different pressures, temperatures and gas mixtures. The ignition process was monitored by observing UV light emission from the OH radicals, which are produced in the non-equilibrium region. Two detectors registered the emission; one detector has been located at end wall and another at side wall of the shock tube.

The ignition delay time must be derived from the time history of an elementary gas volume. The detector, by its nature, collects radiation from a great volume, which consists of elementary volumes with different time histories. Thus, the procedure of the  $\tau_{\text{ign}}$  calculation must include a step for conversion of the detector signal to the parameters of an elementary volume. In the work [1], this step is absent and the raw detector signals were used directly for calculation of the ignition delay times. This procedure is not always correct and can result in errors.

Below, reflected shocks propagated in mixtures of inert gas with a small amount of chemically reactive substances are considered. The integral equations that relate detector signals with intensity radiation of the shocked gas are derived. Solutions of the equations were obtained for the transparent gas. The solutions were compared to signals of sidewall and endwall detectors from [1]; a good agreement has been achieved. The results testify that the suggested technique can be successfully used. These results also show that the use of raw signals of detectors instead of calculated radiation intensity can cause errors in definition of the gas parameters.

## 2. Shock Wave Structure

Structure of reflected shock wave generated in a shock tube facility is shown schematically in Fig.1a for laboratory-fixed coordinates. Let an incident shock propagate from left to right in a test gas mixture at the shock parameters: velocity  $V_2$ , pressure  $P_2$  and temperature  $T_2$ . When the incident shock arrives at the end wall of the tube, a reflected shock starts to be formed. The reflected shock moves from right to left with velocity  $V_{rs}$ . The gas immediately behind reflected shock has parameters  $V_5$ ,  $P_5$ ,  $T_5$ , which are related with  $V_2$ ,  $P_2$ ,  $T_2$  by the Renkin-Hugoniot equations. The gas behind the reflected shock isn't at equilibrium state.

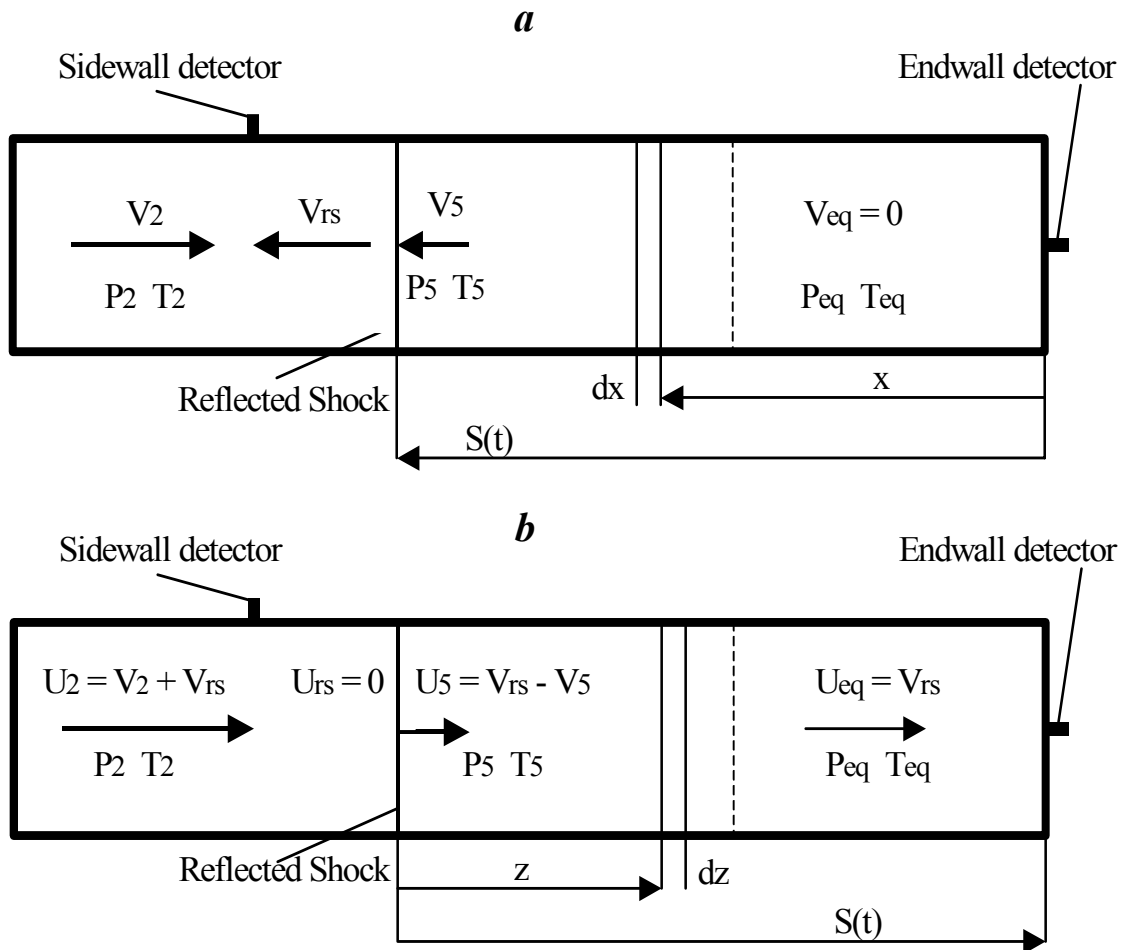


Fig. 1. Reflected shock structure  
*a* - laboratory-fixed coordinates, *b* - reflected-shock-fixed coordinates

That gives rise to chemical reactions and thereby forms the non-equilibrium region. If the reflected shock exists long enough, an equilibrium region develops after the non-equilibrium region. We can identify the structure of the non-equilibrium region in details and consider induction zone and burning zone. Nevertheless, this detailed description will not be used and here we note only the following feature. The gas velocity of the equilibrium region is equal to zero, and thus in the non-equilibrium region the gas velocity varies from  $V_5$  to 0.

Below the reflected-shock-fixed coordinates will be also employed, Fig. 1*b*. We believe that the notations of parameters are clear and do not require additional explanations. Here we only note that the longitudinal coordinate  $z$  has origin at the reflected shock and is directed to the end wall.

In the following consideration we will believe that the reflected shock propagates with constant velocity ( $V_{rs} = \text{constant}$ ) and there are no variations of the gas parameters in the transverse direction.

### 3. Gas-particle Time and Laboratory Time

The goal of experimental works with using shock tube facility is the examination of details of reaction kinetics or determination of global characteristics of reacting systems (for example, ignition delay times). All the mentioned processes take place in shock-heated test gas and essentially are transient. The transient processes occur in time and, therefore, must be referred to a time coordinate. For the reflected shocks, the natural coordinates are the reflected-shock-fixed coordinates. Time related to these coordinates is called gas-particle time. The gas-particle time  $t_p$  is a time required for a gas particle to travel a distance from shock front to the coordinate  $z$  (Fig. 1*b*). The gas-particle time versus  $z$  can be calculated as

$$t_p = \int_0^z \frac{dz'}{u(z')}, \quad (3.1)$$

where  $u(z)$  is gas velocity behind the shock in the reflected-shock-fixed coordinates;  $u(0) = U_5$  (Fig.1*b*). The  $u(z)$  value can be found from mass continuity equation

$$\rho(z) u(z) = \rho_{eq} U_{eq}, \quad (3.2)$$

where  $\rho(z)$  is the gas density behind reflected shock.

The rate processes in the test gas with respect to the gas-particle time  $t_p$  are of the research interest. Nevertheless, all information obtained with the wall detectors (Fig.1*a*) is a function of laboratory time  $t$ . The relation between  $t_p$  and  $t$  can be derived.

$$\frac{dt}{dt_p} = \frac{u(z)}{V_{rs}} \quad (3.3)$$

Usually the equation (3.3) is included in the full set of equations of the reflected shock. The numerical solution of the set gives the test gas parameters (temperature, pressure, species concentrations) as functions

of the gas-particle time  $t_p$ . In this case, the laboratory time  $t$  is used as an independent variable. Generally, the relation between gas-particle time and laboratory time is nonlinear due to the gas movement in the non-equilibrium region ( $u(z) \neq \text{constant}$ ).

In this work, the set of equations will not be solved. We will consider a special case when the test mixture consists of inert gas with small additives of chemically reactive substances. In this case, the gas parameters behind shock vary slightly and we can take  $\rho(z) \approx \rho_{eq}$ . Then Eq.(3.2) gives  $u(z) \approx U_{eq}$  (including  $U_5 \approx U_{eq}$ ). Put very simply, we assume that the gas behind reflected shock has a constant velocity  $U_{eq}$  in reflected-shock-fixed coordinates. Then the right hand side of Eq.(3.3) is close to 1 due to  $U_{eq} = V_{rs}$  (Fig. 1b). Note that in laboratory-fixed coordinates, this assumption corresponds to neglecting the gas movement in the non-equilibrium region, that is, the gas behind reflected shock is at rest,  $V_5 = V_{eq} = 0$  (Fig. 1a).

The solution of Eq. (3.3), where the right hand side is 1, can be written as

$$t_p = t + g(x), \quad (3.4)$$

where  $g(x)$  is an arbitrary function of  $x$ . We can specify  $g(x) = -x / V_{rs}$ . Then the relation between  $t_p$  and  $t$  is

$$t_p = t - x / V_{rs}. \quad (3.5)$$

The Eq.(3.5) has clear physical meaning. If a gas particle is located at an  $x$ -coordinate, then the time history of this particle begins after arrival of the reflected shock at the  $x$ - coordinate ( $t_p \geq 0$  when  $x \leq S(t)$ , Fig. 1a).

If the non-equilibrium region behind shock exists and, nevertheless, we want to use the approach of Eq.(3.5), then an error occurs in calculation of time intervals. The maximal error can be estimated as

$$\varepsilon < \text{abs} \left( \frac{\rho_{eq} - \rho_5}{\rho_{eq}} \right), \quad (3.6)$$

where  $\rho_5$  is the gas density immediately behind reflected shock.

#### 4. Intensity of Gas Radiation

We will consider a small volume of shocked gas, whose parameters are changed due to chemical reactions. The volume is small enough to believe that its parameters are uniform. As a result of chemical processes, excited molecules can be produced. The radiation intensity of these molecules can be calculated as

$$I(t_p) = hv \cdot A \cdot C^*(t_p), \quad (4.1)$$

where  $A$  is transition probability,  $hv$  is photon energy,  $C^*(t_p)$  is the emitted state concentration,  $I(t_p)$  is radiation intensity in the units of (W /cm<sup>3</sup> sr). If the radiation sources are short-lived radicals that are

produced in the non-equilibrium region, the  $I(t_p)$  profile has bell-shaped appearance with a sharp maximum and rapidly decreasing wings. We will call this profile as  $\varphi(t_p)$  (Fig. 2).

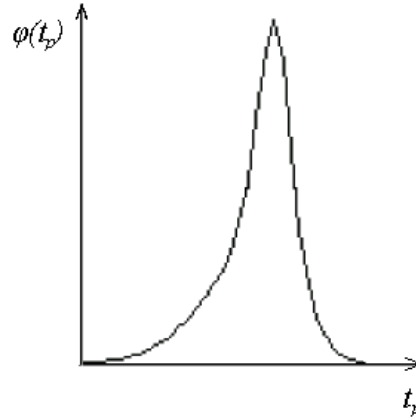


Fig.2. Radiation intensity profile in gas-particle time

Remark -----

Molecular spectra have a very complex structure consisting of many spectral lines. Because of this, general description of radiation processes in molecular gas must be made in terms of frequency integrals. This description isn't used here. In Eq. (4.1) and in the following equations, it is supposed that the radiation parameters are values averaged over a narrow frequency interval. The net results of this work were obtained for transparent gas where the approach of averaged values is absolutely correct. Note that the detectors, used for monitoring emission of shocked gas, work as a rule in narrow frequency intervals as well.

Remark -----

We can more exactly define the bell-shaped function, introducing shape parameters, such as half-width, location of maximum  $t_{p,max}$  and so on. However, below this detailed description is not used and only one feature of the function will be required. We will believe that the integral of the full bell-shaped function with respect to  $t_p$  doesn't depend on the  $t_{p,max}$ , that is, a shift of the function along  $t_p$ -axis doesn't change the integral. The Gaussian function is an example of the bell-shaped function.

$$G(t) = g \exp\left(-\frac{(t - t_m)^2}{a^2}\right)$$

We call attention to the fact that the radiation intensity  $\varphi(t_p)$  (Fig.2) and the concentration  $C^*(t_p)$  (Eq. 4.1) are functions of gas-particle time  $t_p$ . They are just the functions that must be derived from the detector signals in order to calculate the test gas parameters.

Now we must relate the radiation intensity  $I(x,t)$  in the laboratory time with the radiation intensity  $\varphi(t_p)$  in gas-particle time. The assumption that the test gas behind reflected shock is at rest (Section 3) will be used here. In the context of this assumption the laboratory time and gas-particle time are related by Eq. (3.5). Then the expression for radiation intensity  $I(x,t)$  can be immediately obtained substituting  $t$  from Eq. (3.5) for  $t_p$  in the function  $\varphi(t_p)$ .

$$I(x,t) = \varphi\left(t - \frac{x}{V_{rs}}\right), \quad t \geq \frac{x}{V_{rs}}, \quad (4.2)$$

The  $I(x,t)$  profiles are shown in Fig. 3 for different  $x$ . Each profile has origin at the time  $t_k = x_k / V_{rs}$ , when the shock front arrives at the coordinate  $x_k$ . If the shock propagates with a constant velocity  $V_{rs}$ , then all profiles are identical and coincident with  $\varphi(t_p)$ .

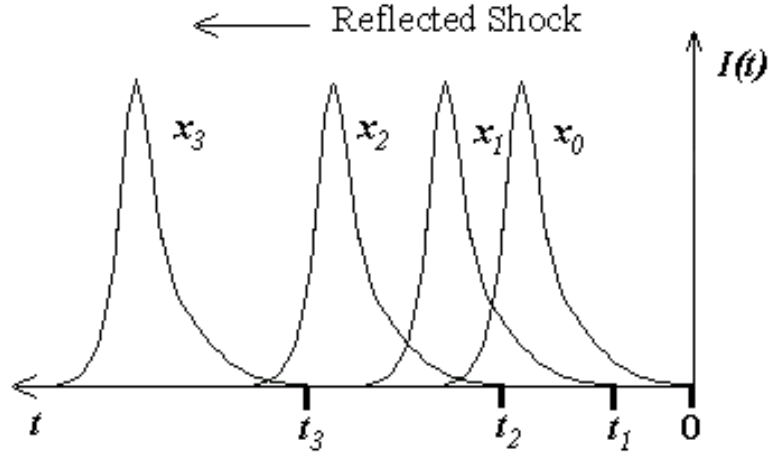


Fig. 3. Radiation intensity profiles in laboratory time for different  $x$ -coordinates

## 5. Endwall Detector

Here we use the results of previous sections in order to relate endwall detector signal with radiation intensity of test gas. The detector signal is proportional to the radiation flux density to the detector surface. The flux is formed by radiation of the shock-heated gas and depends on the longitudinal distribution of radiation intensity  $I(x,t)$  in the shock tube volume. In general form, the relation between the endwall detector signal  $F(t)$  and the radiation intensity  $I(x,t)$  can be written, in view of Eq. (4.2), as:

$$F(t) = c \int_0^{S(t)} \varphi(t - x / V_{rs}) \cdot p(x, t) \cdot dx \quad (5.1)$$

where  $c$  is a parameter that depends on the detector characteristics,  $p(x,t)$  is gas transmittance. The transmittance is defined by gas absorption coefficient and distance from the emitted volume  $dx$  to the detector (Fig. 1a). The transmittance can vary due to variation of gas composition in chemical reactions. The integration with respect to  $x$  is from the end wall ( $x=0$ ) to the shock front ( $x=S(t)$ ).

A qualitative behavior of the endwall signal depending on the gas transmittance is shown in Fig. 4. The profile 1 corresponds to fully transparent gas,  $p(x,t) = 1$ , when radiation of all post-shock region forms the output signal. The profile 3 corresponds to an opaque gas, when only radiation from a region near the end wall achieves the detector. The profile 2 represents the output signal for a weakly absorbed gas. Note that here, as previously, we are dealing with bell-shaped functions of radiation intensity.

The desirable function  $\varphi(t)$  can be found as a result of solution of the integral equation (5.1). For the solution, the exact knowledge of the transmittance  $p(x,t)$  is required and the sophisticated numerical technique must be used. Simplification is possible in the cases of weak gas absorption,  $p(x,t) \approx 1$ . Then Eq. (5.1) can be written as

$$F(t) = c \int_0^{S(t)} \varphi(t - x / V_{rs}) \cdot dx \quad (5.2)$$

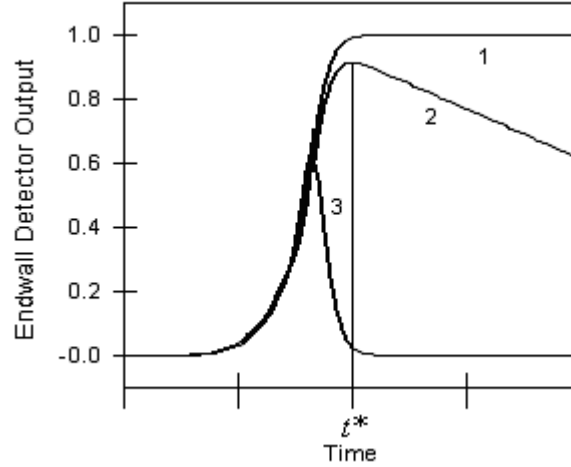


Fig. 4. Output signals of the endwall detector for different gas transparencies

Changing of variables (Eq. 3.5) gives

$$F(t) = cV_{rs} \int_0^t \varphi(t_p) \cdot dt_p \quad (5.3)$$

Solution of Eq. (5.3) gives the required function of the radiation intensity  $\varphi(t)$

$$\varphi(t) \propto \frac{dF(t)}{dt} \quad (5.4)$$

Thus, for transparent gas the radiation intensity  $\varphi(t)$  is proportional to derivative of the endwall detector signal  $F(t)$  with respect to  $t$ .

## 6. Sidewall Detector

The signal  $f(t)$  of the sidewall detector is considered with the assumptions discussed in the previous sections.

$$f(t) = c \int_0^D \varphi(t - x_{sd} / V_{rs}) \cdot p(y, t) \cdot dy \quad (6.1)$$

where  $y$  is the transverse coordinate,  $x_{sd}$  is the longitudinal coordinate of the sidewall detector (Fig. 1a). The integration with respect to  $y$  is from the detector surface ( $y=0$ ) over the shock tube diameter ( $y=D$ ). We assume that the gas in the shock tube is uniform in the radial direction. Then the intensity  $\varphi$  doesn't depend on  $y$  and Eq. (6.1) can be written in the form:

$$f(t_p) = c \varphi(t_p) \int_0^D p(y, t_p) \cdot dy \quad (6.2)$$

Here the relation (3.3) between  $t$  and  $t_p$  has been used.

The radiation intensity  $\varphi(t_p)$  is proportional to the sidewall detector signal  $f(t_p)$ , if the integral in Eq. (6.2) doesn't depend on time. This requirement meets when the transmittance doesn't depend on time, or, in particular, when gas is transparent,  $p(y,t) = 1$ . Then we obtain

$$\varphi(t_p) \propto f(t), \quad t \geq \frac{x_{sd}}{V_{rs}}. \quad (6.3)$$

## 7. Comparison to Experiment

Here the expressions obtained in the previous sections are applied for description of the experimental data from [1]. In the work [1], the ignition process was monitored by observing UV light emission from the OH radicals that are produced in the non-equilibrium region. Two detectors registered the emission; one detector has been located at end wall and another at side wall of the shock tube. The normalized detector signals are presented in Fig. 5 and are denoted as 'Normalized OH\* concentration'. Actually these profiles aren't the OH\* concentration and are only experimental traces, which can be used for calculation of the concentration.

From the shape of the signal of the endwall detector (Fig. 5a) we can conclude that OH\* radiation is weakly absorbed by the gas behind reflected shock (compare with profile 2 in Fig. 3). In this case the Eq. (5.4) can be used to derive the radiation intensity  $\varphi(t)$ . For this purpose the detector signal  $F(t)$  has been approximated by an algebraic function; the function is shown in Fig. 5a and is denoted as "Fit". After differentiating  $F(t)$ , the  $\varphi(t)$  function has been obtained; this function is presented in Fig. 5b and is denoted as "Calculation". The obtained  $\varphi(t)$  function represents truly the OH\* concentration (Eq. 4.1).

As may be seen from Fig. 5b, the calculated function  $\varphi(t)$  is in good agreement with the signal of the sidewall detector. In particular, this coincidence indicates that the absorption of radiation and the gas movement in the non-equilibrium region have a little effect under conditions of Fig. 5. Thus, the radiation intensity  $\varphi(t)$  can be independently derived from signals of the sidewall and endwall detectors.

### Remark -----

The effects of gas movement near the endwall detector are almost always negligible, because during the time interval required for the signal registration (time  $t^*$  in Fig. 2) the equilibrium region is not fully formed.

For the sidewall detector, the effects of gas movement in the non-equilibrium region can be more noticeable. Under conditions of Fig. 5 the time interval error due to gas movement is about 15% (Eq. 3.6). Most likely, this can be a reason for the discrepancy of the calculated and experimental profiles in Fig. 5b.

It should be noted that the gas movement behind reflected shock is a normal consequence of chemical reactions. The effect of this movement on the shock structure depends on intensity of the chemical processes. In mixtures with greater levels of fuel dilution, a steady-state shock with the full shock structure can be formed (Fig. 1). The consideration and conclusions of this work is applicable for these shocks. If the dilution level is low, then behind shock the conditions for transition of the shock wave to a detonation wave can meet. The similar phenomena have been observed and discussed in works [2, 3]. These extremely transient regimes were not considered in the work [1] and are not discussed here.

-----

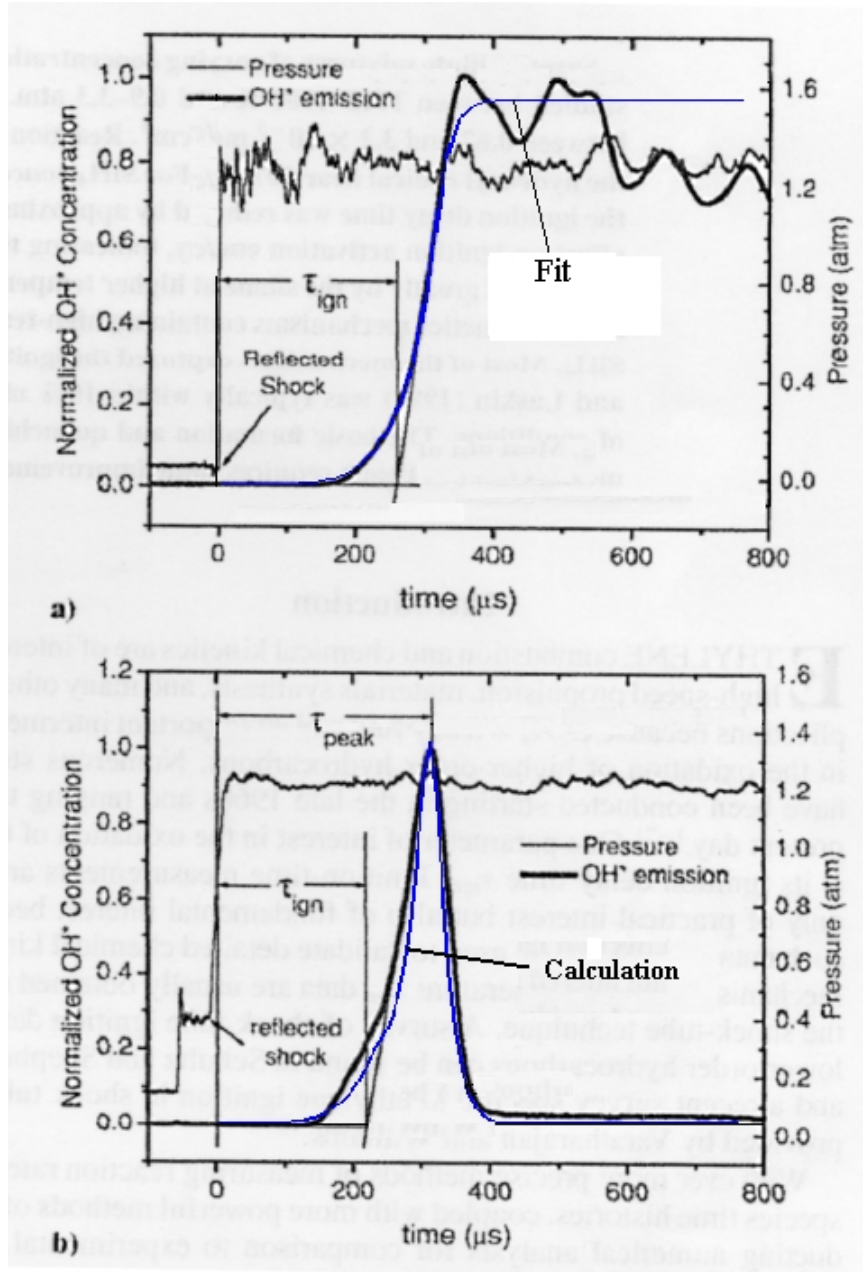


Fig. 5. Reduction of endwall signal to sidewall signal  
 Experimental data [1], gas mixture  $C_2H_4 - 0.3\%$ ,  $O_2 - 1.7\%$ ,  $Ar - 98\%$ ,  $P_5 = 1.23$  atm,  $T_5 = 1404$  K.  
 The traces are the output signals of endwall (a) and sidewall (b) detectors.

## 8. Calculating Ignition Delay Times

As is shown above, only the radiation intensity  $\varphi(t)$  carries information about the time history of an elementary gas volume. This function must be employed for calculating ignition delay times  $\tau_{ign}$  with using, for example, the  $\tau_{ign}$  definition of Fig. 5b. If the sidewall signal is adjusted for the gas movement in the non-equilibrium region, then, ideally, the functions  $\varphi(t)$  obtained from the sidewall and endwall detectors must be identical. In this case, the  $\tau_{ign}$  values calculated from both detectors are identical as well.

In the work [1], the raw detector signals were used directly for calculation of the ignition delay times, as shown in Fig. 5a and b. The Fig. 6 shows typical results obtained simultaneously for both detectors. There are conditions when the signal of sidewall detector approximates the time history of OH\* concentration in an elementary gas volume. In this case the lower curve in Fig. 6 can be defined as ignition delay time.

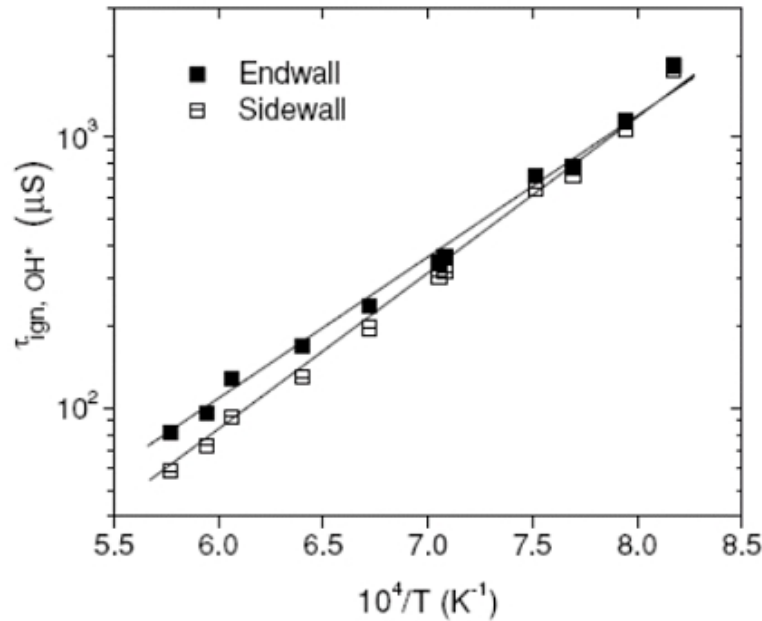


Fig.6. Ignition delay times obtained from sidewall and endwall detector signals. Experimental data [1], gas mixture C<sub>2</sub>H<sub>4</sub> – 0.5%, O<sub>2</sub> – 1.5 %, Ar – 98%, P<sub>5</sub> = 1.07 atm.

The signal of endwall detector represents a time history of the entire shocked gas volume. For this reason, the upper curve in Fig.6 is a characteristic of a great non-uniform gas volume, not an elementary volume, and this curve cannot be considered as ignition delay time.

The authors [1] have admitted the  $\tau_{ign}$  values from the endwall detector as more correct ones without strong proof. Because of this, the ignition delay times  $\tau_{ign}$  and their correlations recommended in [1] are erroneous. We cannot estimate the errors due to the lack of source information; only the authors [1] have these data. However, we believe that the maximum errors of the  $\tau_{ign}$  values can be several tens of percents. The results [1] on the testing of reaction mechanisms are doubtful as well because they are based on the erroneous  $\tau_{ign}$  values.

In the conclusion of this section we note that nowadays there are numeric methods for modeling combustion chemistry. Numeric models can employ detailed reaction mechanisms consisting of hundreds reactions. The methods allow users to predict the parameters of combustion systems (including ignition delay times) with a good accuracy. An example of the numeric calculation for conditions of the work [1] can be found at [4].

## 9. Conclusion

A method for monitoring ignition processes in shock-heated gas mixtures using emission of radicals is discussed. Integral equations, which relate radiation intensity of the radicals with signals of detectors, are presented. Simple solutions of the equations were obtained for case of transparent gas. These solutions were tested against detector signals from work [1]; a good agreement has been achieved. The solutions testify that the use of raw signals of detectors instead of calculated radiation intensity can cause errors in definitions of ignition delay times. For this reason, the results of the work [1], where the ignition delay times are derived from raw signals, are in errors.

## References

- [1] D. M. Kalitan, J. M. Hall and E. L. Petersen. "Ignition and oxidation of Ethylene-Oxygen-diluent mixtures with and without silane", *Journal of Propulsion and Power* **21**, No. 6, pp 1045 – 1056, (2005)
- [2] E. L. Petersen, D. F. Davidson, and R. K. Hanson, "Ignition Delay Times of Ram Accelerator CH<sub>4</sub>/O<sub>2</sub>/Diluent Mixtures", *Journal of Propulsion and Power*, **15**, No. 1, pp. 82–91 (1999).
- [3] D. C. Horning, D. F. Davidson, and R. K. Hanson. "Study of the high-temperature autoignition of n-Alkane/O<sub>2</sub>/Ar mixtures," *Journal of Propulsion and Power*, **18**, No. 2, pp. 363–371 (2002).
- [4] M. Jelezniak and I. Jelezniak.. "CHEMKED – A program for chemical kinetics of gas-phase reactions. Reduced reaction kinetics", (2006).  
[http://mark.jelezniak.de/chemical\\_reactions/samples\\_red.pdf](http://mark.jelezniak.de/chemical_reactions/samples_red.pdf)